Aust. J. Phys., 1995, **48**, 453–60

Electrical Breakdown in Air and in SF_6*

R. Morrow and J. J. Lowke

Division of Applied Physics, CSIRO,
PO Box 218, Lindfield, NSW 2070, Australia.

Abstract

A theory is presented for the development of streamers from a positive point in atmospheric air. The continuity equations for electrons, positive ions, and negative ions are solved simultaneously with Poisson's equation. For an applied voltage of 20 kV across a 20 mm gap, streamers are predicted to cross the gap in 26 ns, and the calculated streamer velocities are in fair agreement with experiment. When the gap is increased to 50 mm for the same voltage, the streamer is predicted not to reach the cathode. In this case an intense electric field front rapidly propagates about 35 mm into the gap in 200 ns. For a further $9 \cdot 5$ μs the streamer slowly moves into the gap, until the electric field at the head of the streamer collapses, and the streamer front stops moving. Finally, only positive space-charge remains; this moves away from the point, allowing the field near the point to recover, giving rise to a secondary discharge near the anode. The electric field distribution is shown to be quite different from that found previously for SF_6; this is explained by the much lower attachment coefficient in air compared with that in SF_6. These results show that streamers in air have a far greater range than streamers in SF_6. This greater range cannot be explained by comparison of the values of E^*, the electric field at which ionisation equals attachment.

1. Introduction

Air and SF_6 are both used as electrical insulating gases. In both gases the sequence of events leading to electrical breakdown is: (1) the formation of an electron avalanche with sufficient space-charge to distort the electric field and initiate streamer formation; (2) the propagation of a streamer all the way across the gap between the electrodes; and (3) the heating of the gas in the streamer channel to form a highly conducting channel which will either lead to the formation of a high current electric arc, or the collapse of the gap voltage if the power supply cannot provide the large current required for an arc.

The relative dielectric strengths of each gas are generally discussed by: (1) comparing their material properties in each gas, for example, the balance between ionisation rates and attachment rates; or (2) by examining the dynamics of the formation of a critical avalanche which leads to the formation of streamers (Pedesen 1970). However, the actual dynamics of streamer propagation are quite

* Refereed paper based on a presentation to the Third Japan–Australia Workshop on Gaseous Electronics and Its Applications, held at Yeppoon, Queensland, in July 1994.

0004-9506/95/030453$05.00

different in each gas, and far greater insight is obtained by comparing the streamer mechanism in air with that in SF_6.

When a positive voltage, applied to a wire in air, is increased slowly, the first corona phenomena observed are short positive onset streamers confined close to the wire, followed rapidly by the formation of the 'Hermstein Glow' (Cross and Beattie 1980), an apparently continuous glow corona uniformly covering the wire. However, when the positive voltage is raised on a sub-microsecond time scale, the onset streamers grow into full streamers which can propagate all the way across the gap. This streamer channel bridging the gap can rapidly become a highly conducting spark which leads to complete electrical breakdown (Marode *et al.* 1979). It is this kind of streamer which is used to remove pollutants from flue gases (Masuda and Nakao 1990). Similar streamer phenomena occur in SF_6 in response to dc and impulse applied voltages (Ibraham and Farish 1980; Wiegart *et al.* 1988).

A theory is presented for the development of streamers from the positive point of a point–plane gap in air at atmospheric pressure, and a comparison is made with previous results for SF_6. Two cases are presented for air, one in which the streamer crosses the gap to the cathode, and a second case in which the streamer fails to reach the cathode. Both cases agree well with available experimental data, and reveal new features of streamer physics; in particular, the range of streamers in air is found to be far greater than in SF_6 due to the effect of attachment on the electric field distribution in the streamer channel.

2. Theory

The streamers are constrained to move down a 100 μm channel, allowing one-dimensional electron and ion dynamics to be used, while the electric field is computed in two dimensions by solving Poisson's equation. The electron, positive ion and negative ion continuity equations, including ionisation, attachment, recombination and photoionisation are solved simultaneously with Poisson's equation to give distributions of electron and ion densities and of the electric field.

The coupled continuity equations for electrons, positive ions, and negative ions are:

$$\frac{\partial N_e}{\partial t} = S + N_e\alpha|W_e| - N_e\eta|W_e| - N_eN_p\beta - \frac{\partial(N_eW_e)}{\partial x} + \frac{\partial}{\partial x}\left(D\frac{\partial N_e}{\partial x}\right), \quad (1)$$

$$\frac{\partial N_p}{\partial t} = S + N_e\alpha|W_e| - N_eN_p\beta - N_nN_p\beta - \frac{\partial(N_pW_p)}{\partial x}, \quad (2)$$

$$\frac{\partial N_n}{\partial t} = N_e\eta|W_e| - N_nN_p\beta - \frac{\partial(N_nW_n)}{\partial x}, \quad (3)$$

where t is the time, x is the distance from the anode, and N_e, N_p and N_n are the electron, positive-ion and negative-ion densities respectively, while W_e, W_p and W_n are the electron, positive-ion and negative-ion drift velocities respectively. The symbols α, η, β and D denote the ionisation, attachment, recombination and electron diffusion. The term S is the source term due to photoionisation.

Poisson's equation is

$$\nabla \cdot E = \frac{e}{\epsilon}(N_p - N_e - N_n)\,, \tag{4}$$

where ϵ is the dielectric constant, and e the electron charge.

The data for the material properties of air and of flue gas mixtures (i.e. α, η, W_e, D) come from our own calculations (Lowke and Morrow 1995). We find that differences in the material functions between air and flue gas are not significant so that our calculations apply equally well to air or flue gas. We use the photoionisation data of Penney and Hummert (1970) for air, and also their method of calculating photoionisation densities (see their equation 2).

The numerical methods used to solve the continuity equations have been described in detail elsewhere (Morrow and Noye 1992; Morrow 1991*a*). However, we have found that serious errors arise from using the disc method (Davies and Evans 1967) to compute the electric field for the case of air with streamers crossing the entire gap. Thus a successive over relaxation (SOR) method has been employed, which like the disc method gives a two-dimensional representation of the electric potential ϕ (with azimuthal symmetry). As with the initial work of Davies *et al.* (1971), our method uses one-dimensional continuity equations with a two-dimensional Poisson equation to give gross features of the physics.

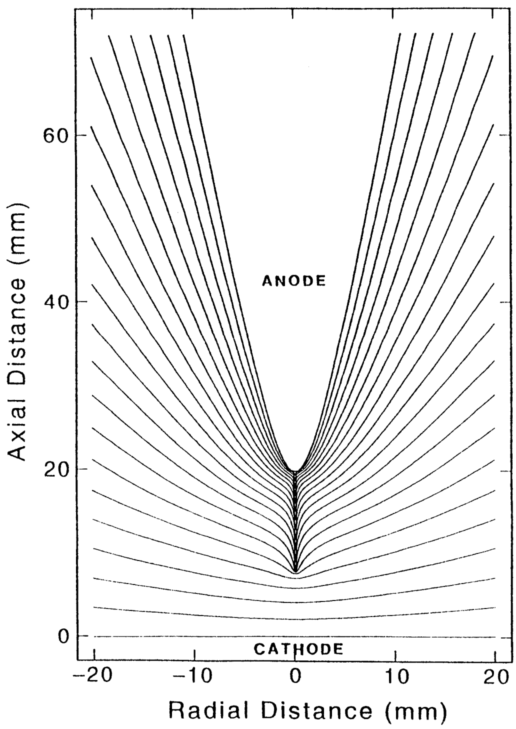

Fig. 1. Equipotential contours, at 1 kV intervals, for a 20 mm gap in air with 20 kV applied, showing the streamer development after 12·5 ns.

3. Results

Results are presented for the development of streamers from the positive point of a point–plane gap in air or flue gas at atmospheric pressure, and these results are compared with results in SF_6 for similar conditions (Morrow 1991*a*, 1991*b*). The point is a hyperboloid with an ~1 mm radius of curvature at the tip. A gap of 20 mm or 50 mm is used, with an applied voltage of 20 kV.

For a 20 mm gap streamers are initiated by the release of ~100 electron–ion pairs near the anode, and within 12·5 ns the streamer develops and is more than halfway across the gap, as shown in Fig. 1; the streamer can be seen to distort the equipotential surfaces as it 'pushes' towards the cathode. The progress of the streamer can be charted by computing the electric field $E = -\nabla\phi$ along the central axis of the system, as shown in Fig. 2. After 26 ns the streamer reaches the anode.

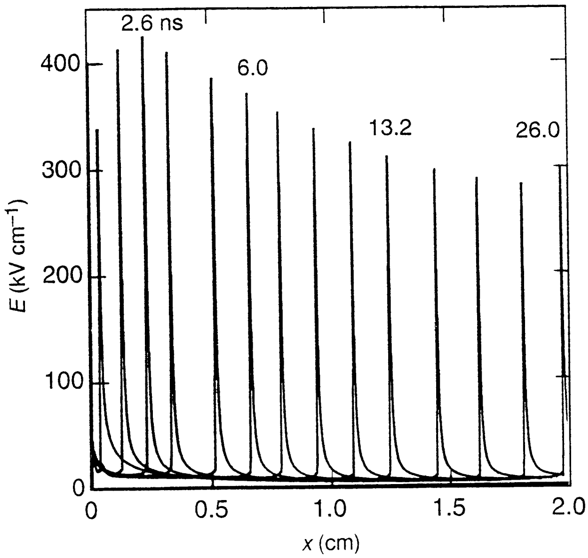

Fig. 2. Electric field distributions computed along the centre line of the potential distributions of the type shown in Fig. 1, at various times shown in ns.

During the streamer's progress the streamer velocity changes considerably, as shown in Fig. 3. These results are in good qualitative agreement with the experimental results of Creyghton *et al.* (1992) (reproduced in Fig. 4) particularly the final velocity of 5×10^5 m s^{-1}. (A separate figure is used for Creyghton's results because the experimental conditions differ significantly from our computational conditions.) Creyghton used two optical fibres at different axial positions to measure the arrival times of the streamer front and thus the streamer velocity.

For a 50 mm gap in air, as shown in Fig. 5, three distinct phases of streamer development can be identified:

(1) a rapid streamer propagation phase, during which an intense electric field front propagates rapidly away from the point into the gap, slows down, and stops about 3·5 cm from the point after 200 ns;

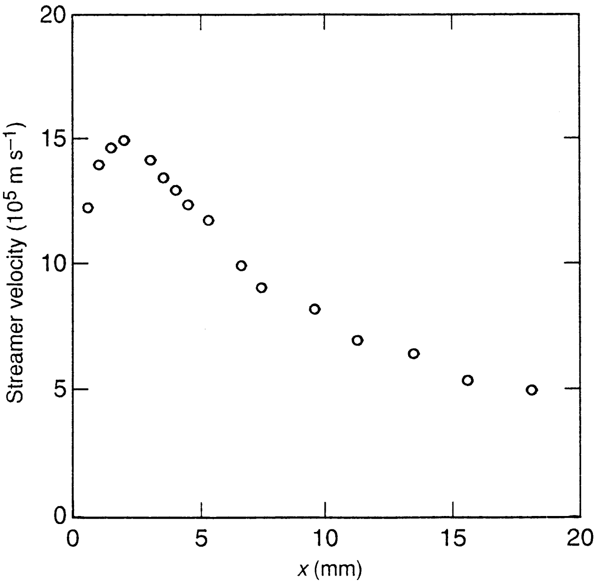

Fig. 3. Computed streamer velocity versus position in air, for a 20 mm gap with 20 kV applied.

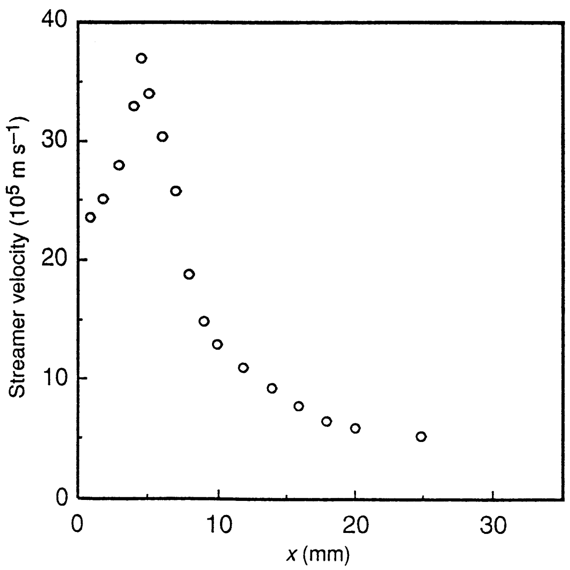

Fig. 4. Measured streamer velocity versus position in air, for a 35 mm gap with 25 kV applied (reproduced from Creyghton *et al.* 1992).

(2) a streamer channel decay phase, during which a slow evolution of electron and ion densities takes place for a further $2 \cdot 0$ μs eventually leaving only a net positive space-charge, accompanied by the gradual collapse of the electric field at the head;

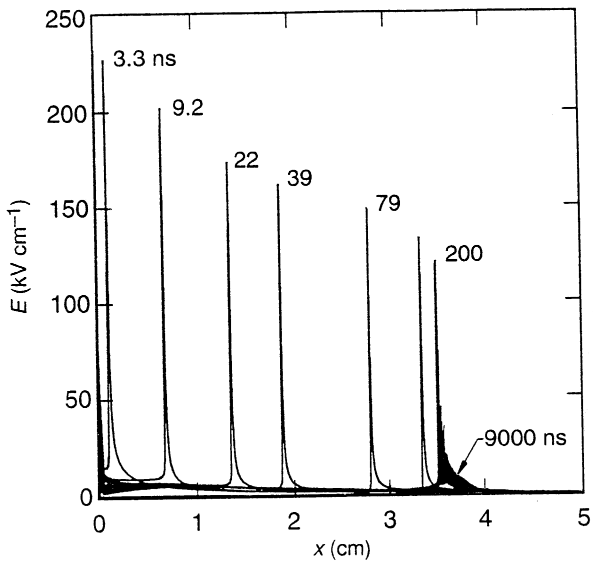

Fig. 5. Electric field distributions at various times in ns, for a 55 mm gap in air with 20 kV applied.

(3) a gap clearing phase, during which positive space-charge moves away from the anode creating the corona wind, and the electric field near the anode begins to rise, leading to the prediction of a secondary discharge near the anode.

Qualitative experiments were performed in our laboratory with the 50 mm point–plane geometry discussed in this paper. A very small sharp point was used at the tip of the electrode in order to regularly trigger streamers (Woolsey 1994). Under the above conditions regular streamers were generated with an applied voltage of ~20 kV, and the streamers were observed to cross ~75% of the gap. With an applied voltage of ~24 kV streamers clearly crossed the entire gap.

The electric field distributions for streamers in air are quite different from those found in SF_6, as shown in Fig. 6 for a 65 mm gap in SF_6, with an impulse voltage of 200 kV applied (Morrow 1991*a*, 1991*b*).

4. Discussion

The results presented in Figs 2 and 3 are in excellent qualitative agreement with the experimental results of Creyghton *et al.* (1992) (for a different geometry and voltage), particularly with regard to the final streamer velocity. The results obtained in our laboratory are only qualitative, but it is clear that for an applied voltage $V > 20$ kV streamers can propagate across more than 50% of the gap, and for $V > 24$ kV the streamer crosses the entire gap. (The need for a sharp point at the tip of the electrode may correspond to our use of a narrow streamer channel for the entire gap.) This gives considerable confidence that most of the dominant physical processes have been taken into account adequately in the model. The structure of the streamer and its dependence on physical parameters can therefore be examined using the model.

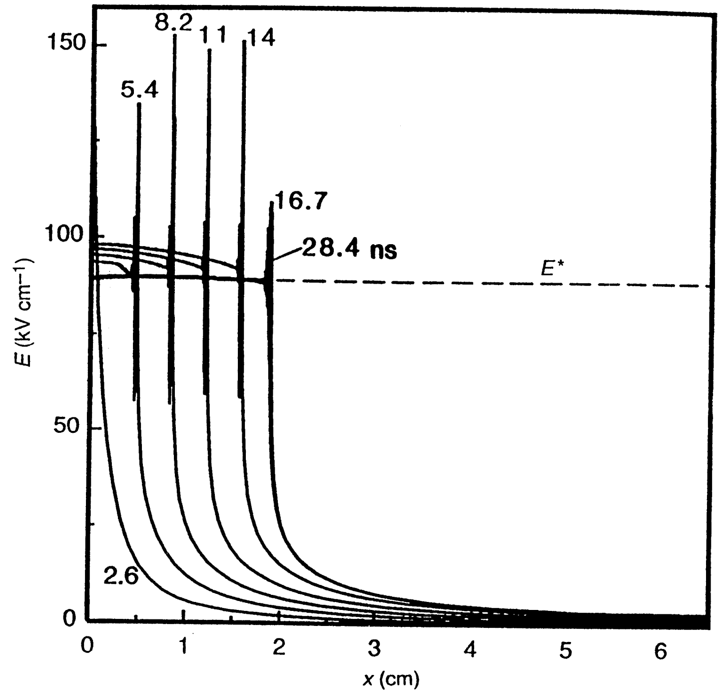

Fig. 6. Electric field distributions at various times in ns, for a 65 mm gap in SF_6, with 200 kV applied.

One factor of particular interest is the dependence of streamer propagation on photoionisation. This is because the electrons move towards the anode, while the streamer head moves towards the cathode, and thus, in the absence of photoionisation, there are no seed electrons in front of the streamer. When the photoionisation coefficients are set to zero, the initial electrons are absorbed into the anode, and no streamer results. Note that dynamic effects such as electron diffusion have been included, and extreme care has been taken in using numerical methods which do not introduce non-physical effects (Morrow and Noye 1992; Morrow 1991*a*). Thus photoionisation is a crucial feedback mechanism placing seed electrons ahead of the streamer front in order for the streamer to propagate.

The most remarkable result is the dramatic difference in the structure of streamers in SF_6 compared with air. For a voltage an order of magnitude higher in SF_6 the streamer penetrates only half as far into the gap, compared with air. For a voltage of 50 kV across a similar gap in SF_6 the streamer penetrates about 3·5 mm (Morrow 1991*a*), compared with about 35 mm for an applied voltage of 20 kV in air. It was shown that in SF_6 the streamer channel must maintain the electric field at a value close to E^* (the field at which ionisation equals attachment $E^* \sim 90\,\mathrm{kV\,cm^{-1}}$ at 1 atmosphere), in order that the gas remain conducting while the streamer is propagating and current is flowing in the circuit (Morrow 1987). This is because electron attachment is so strong in SF_6. In air the restriction that $E \sim E^*$ should not apply because of the weaker attachment in air ($E^* \sim 30\,\mathrm{kV\,cm^{-1}}$ at 1 atmosphere) (Morrow 1987). For example, the attachment time constant for air at $E = 10$ kV, and atmospheric pressure, is

$\tau = 1/\eta W_e \sim 100$ ns, which is far greater than typical times for the formation of streamer channels in air. Thus attachment in air is far too slow to affect the streamer dynamics, and the range of streamers in air is far greater than in SF_6.

5. Conclusions

Streamer propagation in air and flue gas mixtures can be described with a relatively simple model which elucidates most of the experimentally observed properties. In both air and SF_6 a computation is given of a streamer which propagates part way across a breakdown gap and stalls. It has been shown that when computing the insulating properties of air and SF_6, it is not adequate to simply compare relative values of the critical field for which ionisation equals attachment; it is necessary to model the discharge in order to determine if the gap will be bridged by plasma, and therefore break down.

References

Creyghton, Y., Smeets, B., van Veldhuizen, E. M., and Rutgers, W. R. (1992). Proc. Tenth Int. Conf. on Gas Discharges and their Applications, Swansea (Ed. W. T. Williams), p. 302.

Cross, J., and Beattie, J. (1980). *Can. Elec. Eng. J.* **5**, 22.

Davies, A. J., and Evans, C. J. (1967). *Proc. Inst. Electr. Eng.* **114**, 1547.

Davies, A. J., Davies, C. S., and Evans, C. J. (1971). *Proc. Inst. Electr. Eng.* **118**, 816.

Ibrahim, O. E., and Farish, O. (1980). Sixth Int. Conf. on Gas Discharges and Their Applications (Ed. B. F. Hampton), p. 161 (IEE: London).

Lowke, J. J., and Morrow, R. (1995). *IEEE Trans. Plasma Sci.* (accepted for publication).

Marode, E., Bastien, F., and Bakker, M. (1979). *J. Appl. Phys.* **50**, 140.

Masuda, S., and Nakao, H. (1990). *IEEE Trans. Industry Appl.* **26**, 374.

Morrow, R. (1987). *Phys. Rev.* A **35**, 1778.

Morrow, R. (1991*a*). *IEEE Trans. Elect. Ins.* **26**, 398.

Morrow, R. (1991*b*). *IEEE Trans. Plasma. Sci.* **19**, 86.

Morrow, R., and Noye, J. (1992). *In* 'Computational Techniques and Applications: CTAC91' (Eds B. J. Noye *et al.*) (Aust. Math. Soc.).

Pedesen, A. (1970). *IEEE Trans. Power Appar. Syst.* **PAS-89**, 2043.

Penney, G. W., and Hummert, G. T. (1970). *J. Appl. Phys.* **41**, 572.

Wiegart, N., Niemeyer, F., Pinnekamp, F., Boek, W., Kindersberger, J., Morrow, R., Zaengl, W., Zwicky, M., Gallimberti, I., and Boggs, S. A. (1988). *IEEE Trans. Power Delivery* **3**, 923.

Woolsey, G. A. (1994). personal communication.

Manuscript received 26 July 1994, accepted 1 February 1995